IIETA International Information and Engineering Technology Association
Advancing the World of Information and Engineering

Annales de Chimie - Science des Matériaux
Vol. 48, No. 2, April, 2024, pp. 187-195
Journal homepage: http://iieta.org/journals/acsm

Comparative Analysis of Electrode Type on Microstructure and Mechanical Properties in AISI 5155 Low Alloy Steel Welds

Abdul Sameea Jasim Jilabi

Faculty of Materials Engineering, University of Babylon, Hilla 51001 P.O. Box 4., Iraq

Corresponding Author Email: sameeakilabi@gmail.com

https://doi.org/10.18280/acsm.480205

Received: 13 November 2023
Revised: 13 March 2024
Accepted: 12 April 2024
Available online: 30 April 2024

Keywords:
electrode type, low alloy steels, shielded metal arc welding

ABSTRACT

Recently, low alloy steel types have been widely utilized in the manufacture of many important products, which may be damaged during service and require repair by welding. Shielded metal arc welding of 6 mm thick AISI 5155 low alloy steel plates with different electrodes was employed to examine and compare the microstructure and mechanical properties of the welds. The results showed diverse microstructures over the weld metals. The maximum hardness values across the welds were in the CGHAZ, where the structure contained ferrite and pearlite coarser than that of the base metal. The finest structure was in the inter-critical HAZ, in which the minimum hardness was; where partial spheroidization of pearlite occurred. The average weld metal hardness value, for all welds, was lower than that of the base metal (~465 HV). The highest hardness value was (~337 HV) for the weld produced using the OK48.00 electrode, whilst the maximum tensile strength was (938 MPa) for the weld due to the use of the OK76.18 electrode. The low cost electrode (OK46.00) and the expensive one (OK92.18) gave relatively lower mechanical properties, whereas the optimum properties were achieved as a result of using iron powder low hydrogen covering electrodes (OK48.00 and OK76.18).

1. INTRODUCTION

In the past decades, alloy steels have been developed for several reasons, the most important being to eliminate the limitations of using carbon steels. With carbon steels, it is usually difficult to obtain a tensile strength higher than (700 N/mm²) if toughness and ductility are also required. In addition, carbon steels have poor resistance to corrosion. Steel compositions can be developed by adding several alloying elements of different weight percentages including chromium, nickel, tungsten, cobalt and vanadium. Manganese and silicon, as well as sulphur and phosphorous are also incorporated in larger quantities compared to carbon steels [1, 2]. The function of these additives is mainly to improve the strength of steel and its resistance to heat and corrosion, as well as enhancing ductility, machinability and hardenability. Compared to carbon steels, low alloy steel types typically have greater strength, though their cost is slightly higher. A wide range of industries utilize these steels, including railways, oil and gas pipelines, storage tanks, and heavy-duty vehicles. They are also well-suited for construction panels and the manufacturing of dies and various components for agricultural equipment [3, 4]. These industries may fail under heavy duty and therefore require repair using a viable fusion welding process.

As the weight percentages (wt.%) of carbon and alloying elements increase in low alloy steels, their hardenability thus increases at the expense of decreased weldability. Among welding defects, hot and cold cracking in the weld zone (WZ) and heat affected zone (HAZ) are particularly critical, as the weldability of steels is largely determined by the sensitivity to these cracks [5, 6]. Weld cracking can be prevented employing many different measures, like preheating, postheating, and/or buttering. Implementing these measures is however a waste of money, effort and/or time and is sometimes impractical based on the size and geometry of the pieces being welded [7, 8]. Cold cracks (hydrogen cracking) in low alloy steel welds can be prevented by providing low hydrogen welding conditions and slow cooling rates [2]. However, prohibiting or avoiding hot cracks is still a challenge. One of the most efficient ways to reduce hot cracking in steel welds is adding specific wt.% of nickel to the weld pool, as nickel additives can increase toughness and therefore impact strength of the WZ.

On the other hand, shielded metal arc welding (SMAW) process is globally the most common, accounting for more than half of the overall welding processes in certain countries. Due to its simplicity and versatility, this process is a leader in the repair and maintenance work, and is broadly utilized in steel structures and industrial manufacturing. Given the widespread applications and low cost of equipment, the process is expected to remain popular, mainly in small workshops where automated and semi-automated processes are considered uneconomic and unnecessary. The shielding features of its electrodes make the SMAW process less sensitive to wind flow than gas-shielded arc welding processes [7]. With the SMAW process, the selection of appropriate welding electrodes can play a crucial role in controlling weld defects, mainly cracks, and thus the performance and cost of welds.

AISI 5155 is a low alloy steel that has various applications in the automotive, aerospace, construction, oil and gas industries due to its strength, toughness and corrosion-erosion resistance. SMAW of this type of steel requires very careful selection of the electrode type used among the multiple welding electrodes [9]. The types of electrodes specified in this study were chosen based on their availability and knowledge of their potential use in welding this type of steel [10].

After surveying the former literature, articles [11, 12] were found dealing with the study of the influence of electrode type on the microstructure and mechanical behavior of austenitic stainless steel welds achieved using the SMAW process. Other researches [13-17] have focused on shielded metal arc low carbon steel welds by the use of different electrodes. The significant influence of electrode type and welding current on the microstructure and mechanical properties of these welds has been clearly revealed. In 2018, Winarto et al. [18] investigated the influence of using two types of rutile electrodes (E6013 and E7024) on the mechanical behavior of high-strength, low-alloy AH-36 marine steel welds, which are joined underwater at various electric current values. The outcomes showed that the HAZ hardness values for both electrodes were higher than those of the WZ, which in turn were greater than the hardness of the base metal (BM). Besides, the E6013 electrode gave better tensile properties. Finally, Tahmasebi Manesh and Nasresfahani [19] evaluated in 2021 the microstructural and mechanical behavior of high-strength, low-alloy P460NH steel welds of pressure vessel tanks achieved using the E8018-G electrode. The findings showed that the WZ included the greatest proportion of pearlite (~62%), whereas the BM comprised the greatest proportion (~73%) of ferrite. Correspondingly, the HAZ had the greatest hardness value (298 HV) compared to the softer BM (210 HV). The present article aims to investigate and compare the structure and mechanical behavior of the welds resulting from the use of various electrodes with the SMAW of AISI 5155 low alloy steel.

2. EXPERIMENTAL WORK

2.1 Base metal

Table 1 exhibits the chemical composition of the BM steel alloy used in the present study, conforming to the specifications of American Iron and Steel Institute (AISI) [20]. Chemical composition analysis presents that the composition of the raw material (as an average of three readings) is within the ranges identified by AISI. Table 2 shows some important specifications of the BM used.

2.2 Filler metal

Table 3 shows the specifications of electrodes used as filler metal with the SMAW process according to ESAB [10].

2.3 Welding of low alloy steels

The following procedures as recommended by the AWS were carefully performed before starting the welding process.

1. Removing rust from the piece surfaces by (0.5 mm) from each surface, then cleaning the pieces from oils, grease, chip residues and other contaminants.
2. Drying the welding electrodes by gradually heating in ovens from room temperature to the appropriate drying temperature for the electrodes as recommended by the AWS.
3. Fitting-up the distance between the two plates being welded on (2.5 mm) as in Figure 1, which shows the dimensions of these plates and the weld joint design (square butt).
4. Tack welding the two plates at both ends using the same designated electrode selected for final welding. Any slag formed during tack welding is then removed.
5. Adjusting the welding amperage according to the electrode characteristics (type and size) and welding position. The setting should be within the manufacturer's recommended range for these electrodes.

Shielded metal arc welding for the 6 mm thick tack-welded plates of AISI 5155 low alloy steel has then been achieved on a large steel table on both sides according to AWS. The slag produced on one side was completely removed before welding the other side. Table 4 presents the welding conditions for low alloy steel plates.

2.4 Microscopy

Specimens were prepared for microstructural examination according to standard metallographic procedures (based on ASTM E3-2017 and ASTM E 407-2015) which include the following steps: specimen cutting, wet grinding, mechanical polishing and etching. To achieve the wet grinding process, the specimen surface was exposed to an electrically powered rotating disc equipped with SiC sandpaper of various grit sizes (180, 220, 320, 400, 600, 800, 1000, 1200 and 1500) sequentially. After grinding, mechanical polishing with diamond particle pastes (3, 1, and 0.25 μm grit size) was performed using special cloths mounted on the rotary disc. The function of this step is to eliminate grinding-induced new scratches. Finally, a 2% Nital etching was used to differentiate the phases based on their chemical reactivity.

Specimens were prepared for use with optical microscopy and SEM to recognize the microstructures and topography of the welds. The prepared specimens were also utilized to detect and identify the type, size and location of the probable surface defects across the welds.

2.5 Micro-hardness examination

Vickers micro-hardness examination was executed across the welds (WZ, HAZ and unaffected BM) after grinding and polishing the surfaces being measured. This test was carried out under conditions of a 500 g load for 10 s, with an average of three measurements per point.

2.6 Tension test

Three tensile test specimens from each weld were prepared conforming to the American Standards for Testing of Materials (ASTM) [21] shown in Figure 2. The center-line of the weld was located in the mid of the specimen, and the reported tensile strength was an average value. All specimens were notched in the weld zone with a radius of 2.5 mm to ensure that the fracture occurs in this zone (Figure 3).

Table 1. Chemical composition of the BM steel alloy used in the present study

AISI 5155 Steel	Chemical Composition (wt.%)					
	C	Mn	Si	Cr	P	S
Nominal	0.51-0.59	0.7-0.9	0.15-0.3	0.7-0.9	0.035 max.	0.04 max.
Actual	0.558	0.666	0.237	0.752	0.0105	0.0079

Table 2. Specifications of the BM used in the study

Spec. Symbol (AISI)	Raw Material Shape and Cross Section (mm)	Ultimate Tensile Strength (MPa)	Vickers Hardness (HV)	Raw Material Condition
5155	Plate (7*70)	≧1230	220	Annealed and cold drawn

Table 3. Electrodes specifications according to ESAB [10]

Electrode Ø 3.2mm	Electrode Type	Coating Type	Wire Alloy Type	Typical Properties of the Weld Metal			Typical Composition of the Weld Metal (wt.%)						
				T.S. (MPa)	Y.S. (MPa)	El. (%)	C	Mn	Si	Fe	Mo	Cr	Ni
OK46.00	Rutile	Titania-Potassium	Mild steel	510	400	28	0.08	0.4	0.3	B*	-	-	-
OK48.00	Basic	Iron powder-low hydrogen	Mild steel	540	445	29	0.06	1.1	0.5	B*	-	-	-
OK76.18	Basic	Iron powder-low hydrogen	Low alloy steel 1.25Cr 0.5Mo	620	530	20	0.06	0.7	0.3	B*	0.5	1.3	-
OK63.20	Acid rutile	-	S.S.18Cr12Ni3Mo	580	480	35	0.03	0.8	0.7	B*	2.8	18.5	12.0
OK92.18	Basic	-	Ni> 90%	300	100	12	1.0	0.8	0.6	4.0	-	-	94.0

Table 4. Welding conditions of the low alloy steel plates.

Welding by the / Welding Conditions	OK46.00 Electrode	OK48.00 Electrode	OK76.18 Electrode	OK63.20 Electrode	OK92.18 Electrode
Electrode size (mm)			3.2		
Current type			DCRP		
Position			Flat		
Current value (A)	125	140	130	130	145

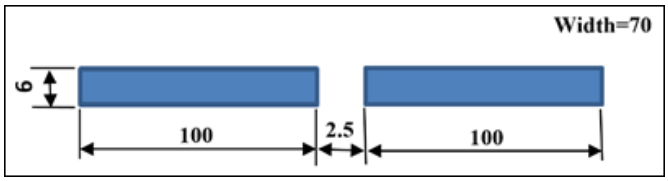

Figure 1. Dimensions (mm) of the plates to be welded

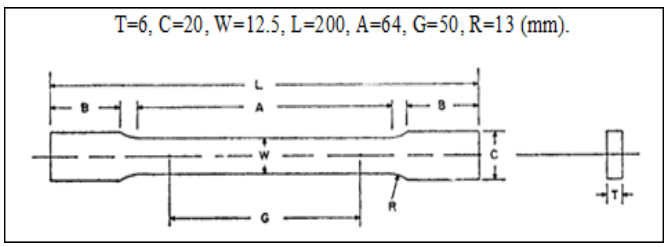

Figure 2. Tensile test specimen based on the ASTM

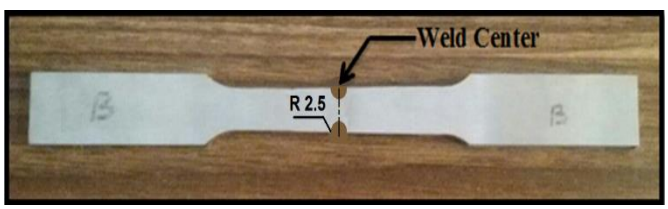

Figure 3. Tensile specimen geometry

3. RESULTS AND DISCUSSION

A square butt weld joint, the most common and widely used design, was chosen as it is suitable for the BM thickness employed in this study according to AWS specifications. In addition, there is no need to prepare the edges of this joint except the conventional cleaning [2].

The microstructural examination of the shielded metal arc AISI 5155 welds made with various electrodes (OK46.00, OK48.00, OK76.18, OK63.20 and OK92.18) revealed three specific regions in each weld: the WZ, the HAZ and the unaffected BM.

Depending on the electrode type used, the microscopic structures of the weld metals varied. This examination also showed variations in the HAZ starting from the vicinity of the WZ (grain growth region) up to that which is unaffected by welding heat, passing through the grain refined and transition regions. These variations are due to the large thermal gradient that the HAZ experiences from the melting temperature to that of the BM unaffected by heat. This is followed by a rapid cooling rate caused by the relatively cold adjacent BM and the atmosphere. This heating and cooling cycle is different heat treatments for each region in the HAZ. As it is known, the difference in the nature of microscopic structures reflects a variation in properties and a difference in performance [2].

Figure 4 illustrates the microstructure of the BM unaffected by welding heat, which comes immediately after the HAZ, displaying primarily a mix of pearlite and ferrite grains in

addition to a very small amount of intergranular pro-eutectoid ferrite depending on the base material's chemical composition and condition (Tables 1 and 2).

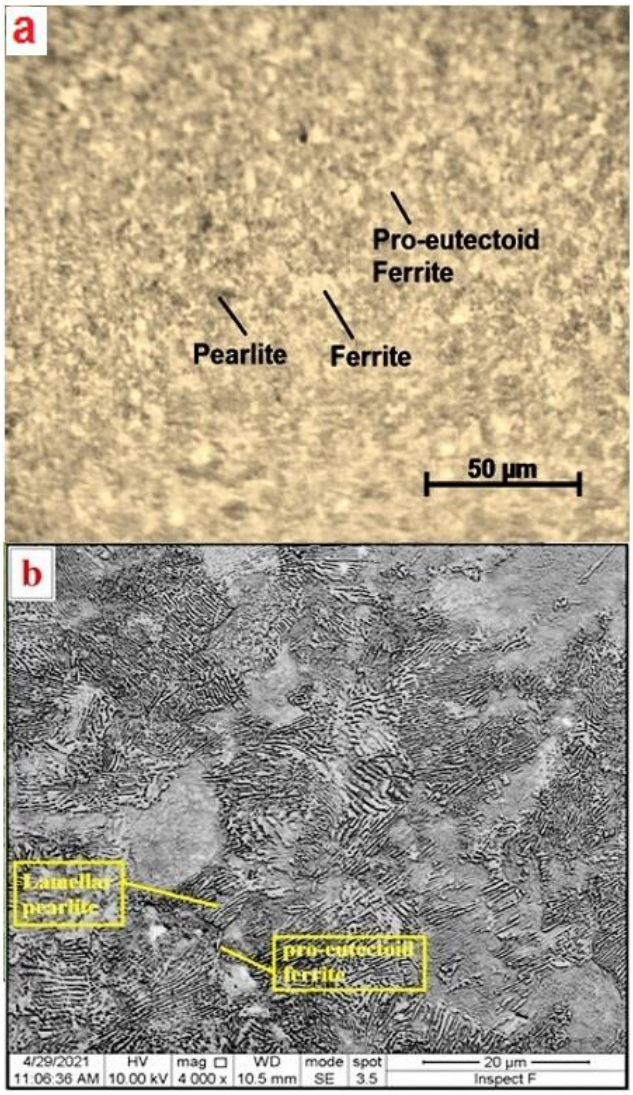

Figure 4. Micrography of the AISI 5155 low alloy steel BM using an (a): OM and (b): SEM

Figure 5 shows that the coarse grain heat affected zone (CGHAZ), the immediate vicinity of the WZ, has a coarsened grain structure. This is due to the higher temperatures to which this region is exposed during welding compared to other regions within the HAZ. The microstructure of this region consists mostly of coarse ferrite and pearlite, and even coarser than those of the BM, as well as a small amount of a needle-like microstructure. The resulting particle size depends on the size of the austenite grains. After welding, this region generally experiences faster cooling rates than other regions within the HAZ, due to the severe thermal drop from the temperature of this region to that of the cold BM [2]. Moving outwards from the center of the weld, the CGHAZ exhibits a progressive decrease in grain size, ultimately reaching the fine grain heat affected zone (FGHAZ). The lower temperature to which this region is exposed results in minimal grain growth, thereby maintaining a fine grain structure. The microstructure of this region shows that the grain size of ferrite and pearlite is finer than that in the BM. However, there are no distinct boundaries between the CGHAZ and the FGHAZ, but rather the grain size changes gradually. The heat treatment to which the grain refined region is subjected is identical to the normalizing heat treatment which is typically applied on carbon steels. The properties of this region are therefore comparable to those of the normalized steel.

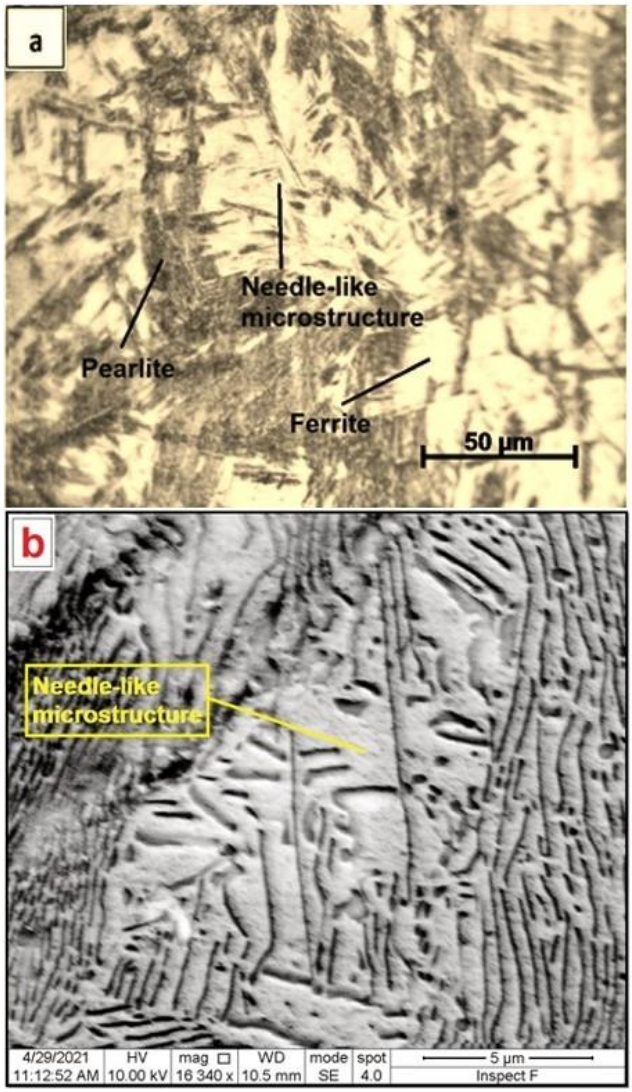

Figure 5. Microstructure of the grain growth region by the use of an (a): OM and (b): SEM

Figure 6 demonstrates the structure of the transition region (Inter-critical HAZ), the region adjacent to the FGHAZ. The finest structure across the welds can be observed in this region, accompanied by partial spheroidization of pearlite colonies. This is consistent with what Hammadi obtained [22].

The HAZ microstructures were similar in all welds, while the microscopy test revealed various structures of the weld metals.

Figure 7 shows that the microstructure of the WZ obtained using the OK46.00 welding electrode was pearlite colonies within a ferrite matrix in addition to a needle-like microstructure which might be a martensitic structure. As expected, the microstructure of the weld produced using the OK46.00 electrode, mainly consists of ferrite and pearlite, since the wire metal type of this electrode is mild steel (Table 3). It is known that the wt.% of the electrode material within the deposited weld metal is the main. However, pearlite appeared in a greater proportion than expected, due to the effect of dilution with the BM, a low alloy steel.

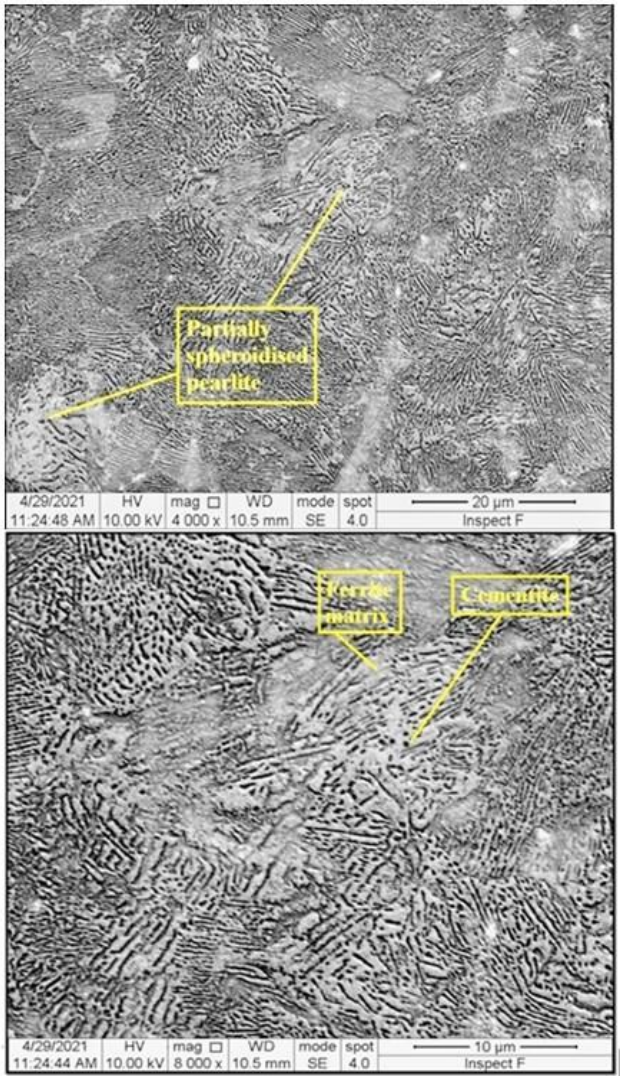

Figure 6. SEM Micrography of the inter-critical HAZ with two magnifications

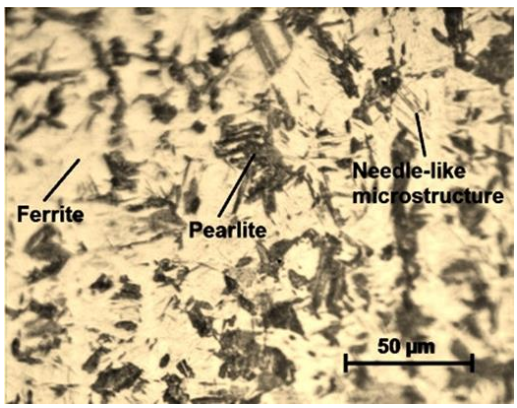

Figure 7. WZ Microstructure of the OK46.00 electrode

Figure 8 clearly illustrates that the microstructure of the weld resulting from the use of the OK48.00 electrode was similar to that of the OK46.00, which mainly consists of ferrite and pearlite, because the electrode wire is also made of mild steel (Table 3).

Figure 9 exhibits that the microstructure of the weld made with the OK76.18 electrode was predominantly acicular ferrite and a small amount of pearlitic structure with intergranular ferrite. This is in agreement with that obtained by Trindade et al. [23] which might be due to the presence of 1.3% Cr and 0.5% Mo in the typical all weld metal composition (Table 3). Due to the fact that the OK63.20 and OK92.18 welding electrodes have relatively high percentages of nickel (Table 3), the microstructures of the weld metals made with these types of electrodes generally seem to be gamma phase only (Figures 10 and 11 respectively). Moreover, during the microscopic examination of the welds, no cracks were observed in the WZ or in the HAZ.

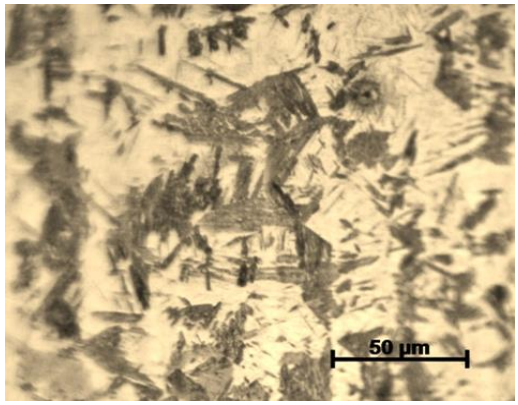

Figure 8. WZ Microstructure of the OK48.00 electrode

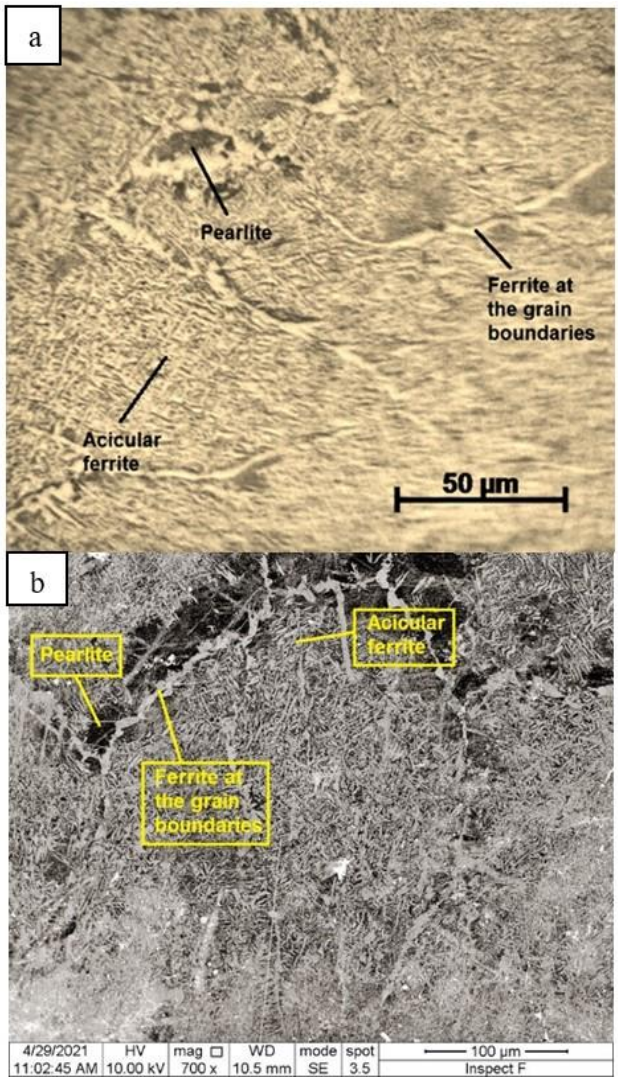

Figure 9. Microstructure of the WZ of the OK76.18 electrode by the use of an (a): OM and (b): SEM

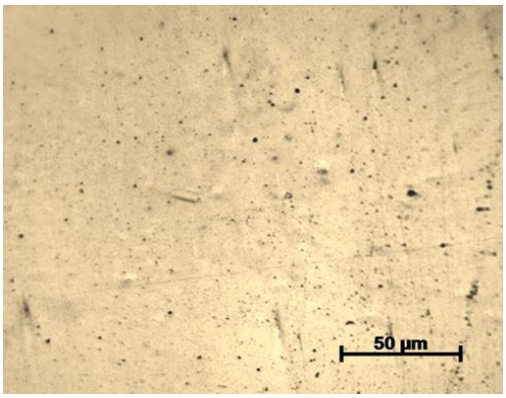

Figure 10. WZ structure of the OK63.20 electrode

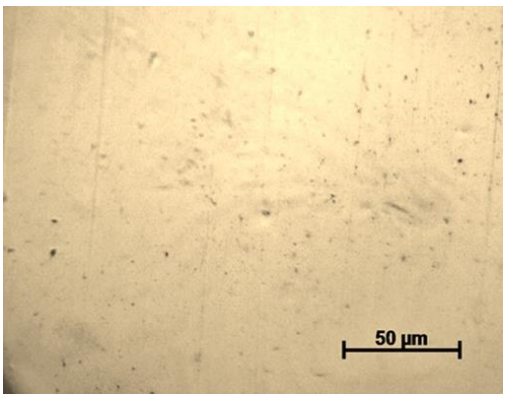

Figure 11. WZ Microstructure of the OK92.18 electrode

Given the series of microstructural variations observed within the welds, it was expected that there would be corresponding variations in hardness as well. Figure 12 shows the hardness variation across the AISI 5155 steel weld (on cross section) made using the OK46.00 electrode. When moving from the center of the weld (1) to the unaffected BM (4), it was observed a sharp increase in hardness value from (~239 HV) reaching to a peak value over the weld (~741 HV) at a distance of 5 mm from the center of the weld (2). The hardness value then decreased significantly to a minimum (~353 HV) at a distance of 12 mm from the center (3). Finally, the hardness gradually increased to that of the BM (~465 HV) at almost 20 mm from the center of the weld (4).

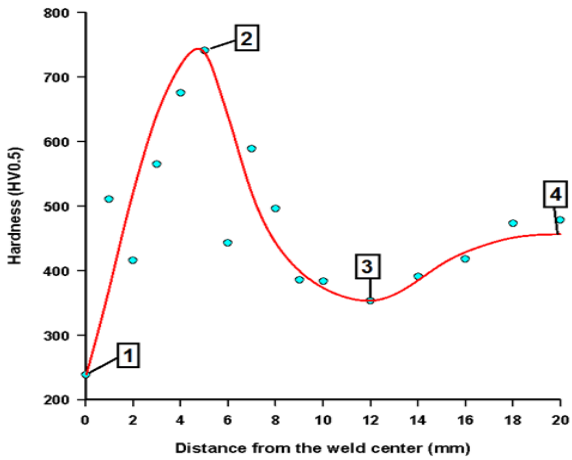

Figure 12. The hardness variation across the center of the weld joined with the OK46.00 electrode, (1): weld center (2): CGHAZ (3): inter-critical HAZ (4): unaffected BM

On average, the hardness at the weld center (1) is lower than that of the BM (4). This could be attributed to the greater proportion of the soft ferrite phase at the center of the weld (Figure 7) as opposed to that in the BM (Figure 4). This variation in structure is because the weld metal typically comprised of both the molten BM and the filler metal produced from mild steel (Table 3). The highest value of hardness across the weld was located at a region close to the center of the weld (2). A possible reason for this rise in hardness is the lower content of the softening ferrite phase within the microstructure observed in this region (Figure 5). On the other hand, this region generally experiences a faster cooling rate compared to the other regions of the HAZ due to the severe temperature gradient between this region and the unaffected BM. Since quicker cooling rates result in smaller interlamellar spacings in pearlite [24], the hardness value is thus higher. This rapid cooling rate might be the reason for the presence of a needle-like microstructure in this region, which may be another cause for this rise in hardness. The minimum hardness across the weld (3), observed in the inter-critical HAZ (Figure 6), likely originated from the presence of a partially spheroidized pearlitic structure in this zone consisting of a partially spheroidized cementite dispersed in a softer ferrite matrix. These findings are generally similar to those obtained by Jilabi [25]. However, the researches [18] and [19] also revealed that the HAZ has exhibited the highest hardness value across the welds.

Figure 13 shows the average hardness values of the welds resulting from the use of the different electrodes (OK46.00, OK48.00, OK76.18, OK63.20 and OK92.18). It is clearly observed that the average hardness value has increased significantly while using the OK48.00 electrode; it is the highest value among the welds. This relatively high value might be due to the manganese content (1.1%) in the weld achieved using this electrode (Table 3). Trindade et al. [23] revealed that manganese has a strong effect in hardening weld metals through solid solutions. The average hardness value due to the use of the OK76.18 electrode has decreased compared to that of OK48.00 owing to the existence of acicular ferrite at the expense of pearlite (Figure 9). Figure 13 also shows that the hardness values have decreased in the welds caused by using the (OK63.20 and OK92.18) electrodes. The reason for these values is the austenitic structure of these welds (Figures 10 and 11) due to the high wt.% of Ni in the typical all weld metal composition (Table 3).

Figure 14 displays the average tensile strength values measured from tensile specimens prepared from the shielded metal arc AISI 5155 steel welds. During tensile testing, the fracture in all specimens was from the WZ, therefore, the measured values indicate the average tensile strength of the weld metals.

It could be noted from Figure 14 that the average tensile strength value of the weld produced using the OK46.00 electrode was (650 MPa). This electrode is specially manufactured for welding mild steel, not low alloy steels, being a cellulosic electrode (high in hydrogen), which exposes hardenable steel welds to cracks of both types, hot and cold. The weld tensile strength thus decreases, as well as promoting the formation of porosity for being high in hydrogen [5, 10, 26]. The OK46.00 electrode was chosen to be used in this research for comparison purposes, due to its cost-effectiveness and wide availability. This is attributed to the high percentage of titania and potassium in the covering of this electrode. These materials are readily ionized under the electric arc's heat,

thus increasing arc stability and facilitating arc initiation during welding [9].

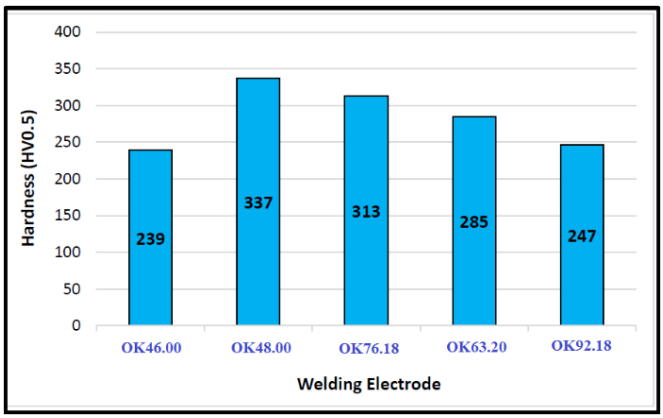

Figure 13. The average hardness in the center of the welds achieved using the different electrodes

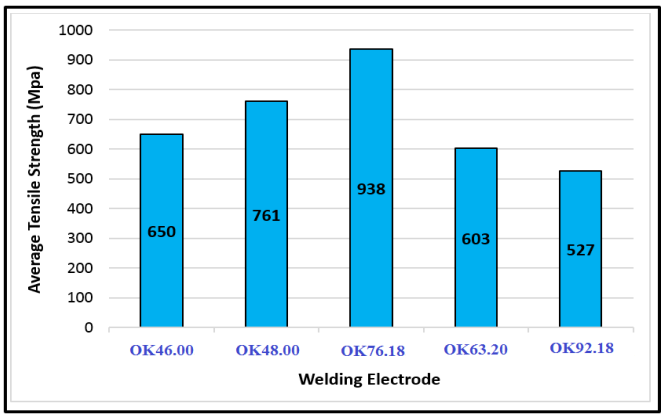

Figure 14. Tensile strength achieved by the welds on average, using the different electrodes

Figure 14 also reveals that the tensile strength of the weld created using the OK48.00 welding electrode was (761 MPa). The wire of this electrode is also made of mild steel, not of low alloy steels (Table 3). As for the relative increase in the value of tensile strength, it might be due to the electrode cover contains a significant percentage of iron powder and low in hydrogen (as evidenced in Table 3). The presence of a large percentage of iron powder (reaching up to 40%), enhances weld deposition rates, and thus reduces dilution, which avoids hot cracks in welds. Moreover, by reason of being low in hydrogen, it reduces the formation of cold cracks, as well as the weld porosity. The weld achieved using this electrode comprises almost (1.1% Mn), which would also enhances the tensile strength of the weld [5, 10, 26, 27].

While using the OK76.18 electrode, it is clear from Figure 14 that the weld tensile strength has increased to (938 MPa). This might be due to the fact that the covering of this electrode is rich in iron powder while maintaining a low hydrogen content (Table 3), thus avoiding weld cracks, both hot and cold, and porosity as well (as mentioned earlier). In addition, the weld achieved using this electrode comprises (1.3% Cr, 0.5% Mo) (Table 3). These alloying elements (as is well known) increase the tensile strength of the weld [1, 10].

When using the OK63.20 electrode, which is specialized for welding austenitic stainless steels, the tensile strength reached by the weld was on average (603 MPa). This relatively moderate value is due to the fact that this electrode is made of austenitic stainless steel, and the austenite is a soft phase. As a result, this property enhances the ductility of the weld and reduces its hardness, thus avoiding cracks in the weld metal [10, 28].

On the other hand, the OK92.18 welding electrode is a nickel electrode specialized for welding cast iron, repairing broken parts and joining parts made of steel, copper or nickel with castings. The weld obtained as a result of using this electrode comprises (Ni≥94 wt.%) [10, 29]. This increases the weld ductility and decreases its brittleness to a large extent, thereby avoiding the occurrence of cracks in cast iron. Figure 14 shows that when this electrode was used for welding the AISI 5155 low alloy steel, the tensile strength was (527 MPa). The specific reason behind this relatively low outcome is that increasing the percentage of nickel by this amount increases the ductility of the weld metal to a very large extent, resulting in lower yield strength and tensile strength of the weld. This is very evident in the fracture zone shown in Figure 15.

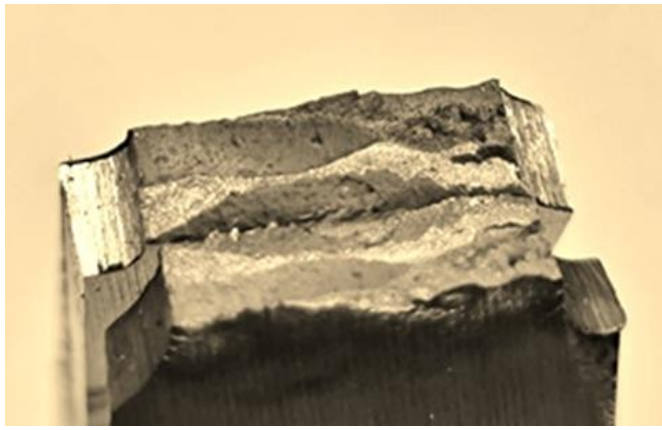

Figure 15. Fractography of the weld produced using the OK92.18 electrode

Table 3 exhibited the typical tensile strength of weld metals achieved using the different welding electrodes in various industrial applications according to ESAB standards. In comparison, the tensile strengths resulting from welding the AISI 5155 low alloy steel using these electrodes were notably higher.

It is worth noting that the prices of the welding electrodes used in this study increase, starting from the OK46.00 to the OK92.18. The increase in welding electrode prices is certainly reflected in an increase in overall welding costs. It is however clear from the results obtained that the use of expensive welding electrodes in welding AISI 5155 low alloy steel did not necessarily lead to an improvement in the resulting mechanical properties, but even led to their decrease in some cases, as is the case when using OK63.20 and OK92.18 electrodes (Figures 13 and 14).

4. CONCLUSIONS

The main conclusions for joining 6 mm thick AISI 5155 steel plates by the SMAW process employing several types of electrodes (OK46.00, OK48.00, OK76.18, OK63.20 and OK92.18) can be drawn as follows:

1. The microstructure of the weld metals ranged from pearlite colonies within a ferrite matrix in addition to a needle-like structure (for OK46.00 and OK48.00) to an austenitic structure (for OK63.20 and OK92.18) passing

through predominantly acicular ferrite and a small amount of pearlitic structure with intergranular ferrite (for OK76.18).

2. The coarsest structure in the HAZ was for all welds in the CGHAZ directly adjacent to the WZ; where the structure contained ferrite and pearlite coarser than that of the BM. The finest structure across the welds was however in the inter-critical HAZ, in which the pearlite was partially spheroidized.
3. The average hardness value of the weld metal, for all welds, was less than that of the BM (~465 HV). The maximum hardness across the welds was in the CGHAZ at a small distance from the center of the weld, whereas the minimum hardness was in the inter-critical HAZ.
4. The highest hardness value of the weld metals was (~337 HV) as a result of using the OK48.00 electrode, whereas the lowest value was (~239 HV) for the weld produced using the OK46.00 welding electrode.
5. The maximum tensile strength was (938 MPa) for the weld due to the use of the OK76.18 electrode, while the minimum value was (527 MPa) for the weld achieved using the OK92.18 electrode.
6. The low cost, commonly used, cellulosic (high hydrogen) welding electrode (OK46.00), and the expensive electrode (OK92.18) gave relatively lower mechanical properties (hardness and tensile strength). These properties notably increased while using iron powder low hydrogen covering electrodes (OK48.00 and OK76.18).
7. The tensile strengths resulting from welding the AISI 5155 low alloy steel using different electrodes were notably higher than typical tensile strengths of weld metals as a result of using the same electrodes in various applications according to ESAB standards.
8. The mechanical properties obtained as a result of using the low cost electrode (OK46.00) could be sufficient for many industrial applications of low alloy steels.

5. RECOMMENDATIONS

There are some suggestions that can be taken into consideration for future work:

1. Other welding processes can be used for comparison, such as SAW, TIG and MIG.
2. The impact test can also be carried out for low alloy steel welds to identify their toughness.
3. Using X-ray radiography to detect the size, number, location and type of some potential internal defects in the welds.

REFERENCES

[1] Bailey, F.W.J. (1972). Fundamentals of Engineering Metallurgy and Materials. 5th ed, Wiley, London.

[2] Khanna, O.P. (1980). Welding Technology: A Textbook for Engineering Students. 1st ed. Dhanpat Rai and Sons, Delhi.

[3] Levy, B.S. (1979). Design and manufacturing guidelines for ultra high strength steel bumper reinforcement beams. SAE Transactions, 88: 1151-1161. https://doi.org/10.4271/790333

[4] Fine, T.E., Dinda, S. (1975). Development of lightweight door intrusion beams utilizing an ultra high strength steel (No. 750222). SAE Technical Paper. https://doi.org/10.4271/750222

[5] Stuart, W.G. (1997). Advanced Welding. 1st ed. Basingstoke: Macmillan.

[6] Lancaster, J.F. (1987). Metallurgy of Welding. 6th ed. Woodhead publishing limited. Cambridge, England.

[7] Davies, A.C. (1989). The Science and Practice of Welding: v. 1. Welding Science and Technology -- v. 2. The Practice of Welding. Cambridge [England]; New York: Cambridge University Press

[8] Welding Training Centre (WTC). (1983). Metallurgical Processes of Arc Welding.

[9] Metals Handbook. (1971). Welding and Brazing. 8th ed. ASM International. Handbook Committee.

[10] ESAB Welding Handbook. (2001). Consumable for Manual and Automatic Welding. 6th ed.

[11] Verma, J., Taiwade, R.V., Khatirkar, R.K., Kumar, A. (2016). A comparative study on the effect of electrode on microstructure and mechanical properties of dissimilar welds of 2205 austeno-ferritic and 316L austenitic stainless steel. Materials Transactions, 57(4): 494-500. https://doi.org/10.2320/matertrans.M2015321

[12] Yousaf, A., Pasha, R.A., Muhammad, A. (2021). Effect of filler materials on mechanical properties of shielded metal arc welded AISI 316L austenitic stainless steel joints. In Icame21, International Conference on Advances in Mechanical Engineering, Pakistan.

[13] Syahroni, N., Rochani, I., Nizar, H. (2006). Experimental study of electrode selection effects on mechanical properties of underwater wet welded-joints. ARPN Journal of Engineering and Applied Sciences, 11(2): 1010-1015.

[14] Tahir, A.M., Lair, N.A.M., Wei, F.J. (2018). Investigation on mechanical properties of welded material under different types of welding filler (shielded metal arc welding). AIP Conference Proceedings, 1958(1): 020003. https://doi.org/10.1063/1.5034534

[15] Nassar, A., Lefta, R., Abdulsada, M. (2018). Experimental study of the effect of welding electrode types on tensile properties of low carbon steel AISI1010. Kufa Journal of Engineering, 9(4): 163-173. https://doi.org/10.30572/2018/KJE/090411

[16] Sumardiyanto, D., Susilowati, S.E. (2019). Effect of welding parameters on mechanical properties of low carbon steel API 5L shielded metal arc welds. American Journal of Materials Science, 9(1): 15-21. https://doi:10.5923/j.materials.20190901.03

[17] Pratomo, M.A., Jasman, J., Erizon, N., Fernanda, Y. (2020). The variation effect of electric current toward tensile strength on low carbon steel welding with electrode E7018. Teknomekanik, 3(1): 9-16. https://doi.org/10.24036/tm.v3i1.5572

[18] Winarto, W., Purnama, D., Churniawan, I. (2018). The effect of different rutile electrodes on mechanical properties of underwater wet welded AH-36 steel plates. AIP Conference Proceedings, 1945(1): 020048. https://doi.org/10.1063/1.5030270

[19] Tahmasebi Manesh, H., Nasresfahani, A. (2021). Evaluation of microstructural properties and investigation of corrosion behavior of P460NH welded steel using E8018-G electrode. Journal of Welding Science and Technology of Iran, 7(1): 89-96.

[20] Spring Steels AISI AISI-5155. (2022). Ju Feng Special Steel Co., Ltd. (jfs-steel.com). https://www.jfs-

steel.com/en/steelDetail/AISI-5155.html.
[21] ASTM International (1989). Metals Test Method and Analytical Procedures. Vol. 03.01. https://www.astm.org/astm-bos-03.01.html.
[22] Hammadi, D.K.Y. (2021). The effect of nickel additions on submerged arc low alloy steel weld. M.Sc. dissertation. University of Babylon.
[23] Trindade, V.B., da Cruz Payão, J., Souza, L.F.G., da Rocha Paranhos, R. (2007). The role of addition of Ni on the microstructure and mechanical behaviour of C-Mn weld metals. Exacta, 5(1): 177-183. https://www.redalyc.org/pdf/810/81050119.pdf.
[24] Gomes, M.D.G.M.D.F., De Almeida, L.H., Gomes, L.C.F.C., Le May, I. (1997). Effects of microstructural parameters on the mechanical properties of eutectoid rail steels. Materials Characterization, 39(1): 1-14. https://doi.org/10.1016/S1044-5803(97)00086-7
[25] Jilabi, A.S.J.A.Z. (2015). Welding of Rail Steels. The University of Manchester (United Kingdom).
[26] Gray, T.G.F., Spence, J. (1982). Rational welding design. Subsequent Edition. London, Boston, Durban.
[27] Sacks, R.J, Bohnart, E.R. (2004). Welding: Principles and Practices. 3rd ed., McGraw-Hill Companies.
[28] ASM Metals Handbook (1975). Failure Analysis and Prevention. 18th ed.
[29] Oerlikon. (2002). Handbook of Welding Consumables. COBISA GmbH Germany.

NOMENCLATURE

El.	elongation, %
T.S.	tensile strength, MPa
wt.	weight percentage, %
Y.S.	yield strength, MPa

Greek symbols

Ø	electrode diameter, mm

Subscripts

AISI	American Iron and Steel Institute
ASTM	American Standards for Testing of Materials
AWS	American Welding Society
CGHAZ	coarse grain heat affected zone
DCRP	direct current reverse polarity
FGHAZ	fine grain heat affected zone
HAZ	heat affected zone
MIG	metal inert gas
OM	optical microscopy
SAW	submerged arc welding
SEM	scanning electron microscopy
SMAW	shielded metal arc welding
TIG	tungsten inert gas
HV	Vickers hardness
WZ	weld zone